The Astrophysical Journal, ???, ???, 2009 January

Testing Formation Mechanisms and Ages of Fossil Groups of Galaxies with Chandra

[1]Dupke, R.A., [2]Mendes de Oliveira, C. & [2]Sodré, L.

[1]Dept. of Astronomy, The University of Michigan, Ann Arbor

[2] Departamento de Astronomia, IAG/USP, Rua do Matão 1226, 05508-090, São Paulo. Brazil

Abstract

Fossil groups are X-ray bright galaxy systems that present an unusual lack of luminous galaxies in the inner regions, except for a giant central galaxy. Recent measurements of galaxy velocity dispersion and X-ray gas temperatures show that they occupy a locus in the L_X-T_X diagram in accordance to those of galaxy clusters. The standard explanation for their formation suggests that bright galaxies within half the virial radii of these systems were wiped out by cannibalism forming the central galaxy. Cosmological simulations indicate that these systems are old, given the high concentration parameters measured in the few fossil groups with enough X-ray counts, and also by the large magnitude gap between the 1st and 2nd rank galaxies, and from the apparently undisturbed X-ray morphologies. One inconsistency with an old age for fossil groups is that, despite the measured short intragroup gas cooling times, they typically do not have cold cores.

Since dry mergers, typically invoked to explain the formation of the central galaxies, are not expected to change the IGM energetics significantly, thus not preventing the formation of cooling cores, we investigate the scenario where recent gaseous (wet) mergers formed the central galaxy injecting energy and changing the chemistry of the IGM in fossil groups. We test here this scenario using fossil groups with enough X-ray flux in the Chandra archive by looking at individual metal abundance ratio distributions near

the core. The results indicate that strong SN II-powered galactic winds resulting from galaxy merging would be trapped by their deep potential wells reducing the central enhancement of SN Ia/SN II iron mass fraction ratio from 99±1% in the outer regions to 85±2% within the cooling radius and would inject enough energy into the IGM preventing central gas cooling. The results are consistent with a scenario of later formation epoch for fossil groups, as they are defined, when compared to galaxy clusters and normal groups. Despite a possible earlier epoch formation for their dark matter haloes, the central galaxy merger that formed the bright group galaxy (BGG) happens at later times in fossil groups than in regular clusters and groups of galaxies.

Subject headings: cooling flows—galaxies: clusters: individual (RXJ1416.4+2315, ESO3060170, RXJ1331.5+1108, NGC6482, RXJ1340.6+4018, RXJ1159+5531)—intergalactic medium—X-rays: galaxies: clusters—galaxies: elliptical and lenticular, cD – galaxies: evolution

1 - Introduction

Fossil groups are classically defined as systems dominated by a single giant elliptical galaxy and with a 2 mag difference between the first and second rank galaxies (in R-band) within 0.5 r_{200}. They are bright sources of extended X-ray emission ($L_{X,bol}>10^{42}\ h_{50}^{-2}$ erg/s). Even though the first of these systems was discovered more than a decade ago (Ponman et al. 1994), their origin and evolution are still strongly debated. This is mostly due to the low number of fossil groups with good quality X-ray and optical data available. Fossil groups were originally thought to be the cannibalistic remains of galaxy groups that lost energy through dynamical friction, perhaps the final stage of compact groups (e.g. Mulchaey & Zabludoff 1999). This idea is consistent with some observational characteristics, e.g., their high X-ray luminosities (L_X), the gap in the luminosity function at L* near the central regions and the strong correlation of total L_X to the optical luminosity of the central bright group galaxy (BGG). Given the expected large times

involved in dynamical friction and the observed lack of X-ray substructures (however, see Zibetti et al. 2009), this model would imply that fossil groups formed early and were undisturbed for a very long time (Ponman et al. 1994; Vikhlinin et al. 1999; Jones et al. 2000).

More recently, X-ray and optical measurements of fossil groups have shown some inconsistencies with this formation mechanism. Firstly, the X-ray measured temperature (T_X) of the fossil group's intergalactic medium (IGM) is similar to that of poor clusters, sometimes in excess of 4 keV (e.g. Khosroshahi et al. 2006a). Recent measurements of galaxy velocity dispersion in fossil groups (Mendes de Oliveira et al. 2006; 2008; Cypriano et al. 2006) seem to be consistent with the T_X measured, at least for the few fossil groups with relatively good X-ray data available, as exemplified by their not atypical location in the L_X-T_X relation (e.g. Khosroshahi et al. 2007). This indicates that fossil groups have relatively deep gravitational potential wells, closer to those of galaxy clusters than to normal groups. The lack of bright galaxies in "cluster-sized" potentials makes these systems unique.

There are also inconsistencies concerning fossil group's formation epochs. On one hand, the X-ray derived mass profiles correspond to very high values of the concentration parameter (c_{200}). Given the correlation found between c_{200} and formation epoch in N-body simulations of ΛCDM cosmologies (Wechsler et al. 2002), fossil groups should be very old ($z_{formation}>1.5$). Additional support for early formation of fossil groups comes from numerical+hydro simulations, which suggest a correlation between formation epoch and magnitude difference of 1st and 2nd brightest galaxies in simulated groups, the older groups having larger magnitude differences (D'onghia et al. 2005). The latter suggests a typical fossil group formation age of ~4.8-6.9 Gyr ($0.75<z<1.3$) as opposed to regular groups ~ 7.2-8.4 Gyr ($0.5<z<0.7$). On the other hand, the cooling time of fossil groups is observed to be significantly less than the Hubble time (e.g., Sun et al. 2004; Khosroshahi et al. 2004, 2006a), but *they typically lack cooling cores*. Heating by AGN activity is unlikely to be the responsible mechanism for this notable difference from poor clusters

and groups of galaxies. There is little sign of AGN activity in the core of fossil groups (X-ray bubbles or arms, strong radio emission, etc.) and AGNs are also ubiquitous in regular groups and poor clusters, which show cooling cores very frequently (e.g. Finoguenov & Ponman 1999; Rasmussen & Ponman 2007), despite their AGN activity. Therefore, the lack of cooling cores in fossil groups would suggest that they were formed "after" regular groups and the IGM did not have time to cool.

In this short paper we place some constraints on fossil group formation models by looking at the IGM chemical history. The elemental abundance for an optically thin plasma can be directly associated to the SN Type enrichment of the gas (Mushotzky et al. 1996). Since SN Ia and II explosions produce different amounts of different elements, the SN Ia and SN II relative contamination in the ICM can be determined through the X-ray measurements of metal abundance ratios. Furthermore, the ratio of SN Ia/SN II pollution in the ICM throughout clusters and groups often shows radial gradients, the central region having a higher value of the Fe mass fraction coming from SN Ia to that of SN II (e.g. Dupke 1999; Dupke & White 2000a,b; Allen et al 2001; Finoguenov et al. 2000; Dupke & Arnaud 2001; Ettori, et al. 2002; de Plaa, J., et al. 2006; Rasmussen & Ponman 2007; Rasera et al. 2008). This implies that metals in the ICM are produced by multiple mechanisms. SN II-powered protogalactic winds and ram-pressure stripping are the most popular mechanisms (although a third mechanism, SN Ia winds, has also been invoked to explain the high SN Ia Fe mass fraction in clusters; see Dupke & White 2001b). These two mechanisms will inject metals with different spatial distributions. While SN II protogalactic winds will disperse metals into the ICM in a more instantaneous and distributed form, ram-pressure stripping should deposit metals in a more centralized way, given its dependence on the gas density (cf. Lagana et al. 2008). The latter would be a slower and continuous process that should increase not just the central Fe abundance but, also the central SN Ia Fe mass fraction with time.

The traditional way to wipe out the bright galaxies in the central regions of fossil groups is through mergers. If (1) fossil groups are older than normal groups and clusters and if (2) the central galaxies in fossil groups were formed by "dry" (gasless) mergers, neither the metal enrichment nor the energetics of the core IGM would be expected to be altered and one should expect to find a cooling core and a central enhancement of SN Ia ejecta as strong (or more) as that found in poor clusters and regular groups. However, recent optical isophotal analysis of the central galaxies of seven bona-fide fossil groups (Khosroshahi, Ponman & Jones 2006b) showed that (at least) six of them had disky isophotes (cf. La Barbera et al. 2009), differently from normal groups (more equal boxy-disky shape distribution) and clusters (biased towards boxier shapes).

Disky isophotes are expected from secondary gas infall (Khochfar & Burkert 2005), suggesting that the merger(s) that created the central galaxies in fossil groups were "wet" (with late-type galaxies). If the destruction of bright galaxies near the core was due to merging and if gas rich galaxies took part in the process, one should expect star formation bursts (e.g. van Dokkum et al. 1999), driving subsequent metal rich SNII-driven galactic winds (e.g. Strickland et al. 2004, Heckman et al. 1990). These secondary winds would deposit metals and energy in the central regions, which could contribute to explain the lack of cooling cores in fossil groups. This secondary wind metal injection would also change the chemistry of the IGM, making the central ratio of SN Ia/SN II Fe mass ejecta in fossil groups lower than that of normal groups and clusters. Here, we investigate this scenario for a sample of six fossil groups observed with the Chandra satellite that satisfy the minimum observational requirements (see below), RXJ1416.4+2315, RXJ1340.5+4017, ESO3060170, RX J1331.5+1108, NGC6482 and RX J1159+5531.

2 – Fossil Group Sample and Data Reduction

As we mentioned in the previous section, in order to carry out ratio abundance measurements we need to be able to spatially resolve X-ray spectra from the inner and outer regions of fossil groups. We selected a sample of six confirmed fossil groups with the minimum number of X-ray counts for such an analysis in the Chandra archive. The observational parameters of the targets are shown in Table 1, where the columns indicate (from left to right) the target names, the Chandra observation IDs, the nominal and effective exposure times, the Chandra detector, the observation date, the J2000 RA and Dec and the target redshifts.

Table1

Target	**ObsID**	**Exp.Time (ksec)/ (Eff. Exp Time)**	**Instrument**	**Obs Time**	**RA**	**Dec**	**Redshift**
RXJ1416.4+2315	2024	15/(14.8)	ACIS-S	Sep 5 2001	14:16:27.10	+23:15:34.60	0.1380
ESO3060170-B	3188	15/(14.1)	ACIS-I	Mar 8 2002	05:40:12.00	-40:51:54.00	0.0358
ESO3060170-A	3189	15/(14.3)	ACIS-I	Mar 9 2002	05:40:07.20	-40:48:00.00	0.0358
RXJ1331.5+1108	3213	31/(25.1)	ACIS-S	Dec 3 2002	13:31:30.20	+11:08:03.00	0.0790
NGC6482	3218	20/(18.2)	ACIS-S	May 20 2002	17:51:48.90	+23:04:19.00	0.0130

RXJ1340.6+4018	3223	50/(47)	ACIS-S	Aug 28 2002	13:40:32.80	+40:17:40.00	0.1710
RXJ1159+5531	4964	80/(75.7)	ACIS-S	Feb 11 2004	11:59:51.40	+55:32:01.00	0.081

All fossil groups were centered on the S3 chip with the exception of ESO3060170, which was observed twice with the I-array (centered on I0 and I3). The individual analysis of that fossil group was carried out using regions of the same size and simultaneously fitting the spectra from both observations. We used Ciao 3.3.0.1 with CALDB 3.2.3 to screen the data. We excluded flare-like periods and the resulting useful exposure times are shown in Table1 (effective exposure time). A gain map correction was applied together with PHA and pixel randomization. ACIS particle background was cleaned as prescribed for VFAINT mode for all fossil groups except for RXJ1416.4+2315, where mode prescription FAINT was used. Point sources were extracted and the background used in spectral fits was generated from blank-sky observations using the acis_bkgrnd_lookup script. Here, we show the results of spectral fittings with XSPEC V11.3.1 (Arnaud 1996) using the *apec* and *Vapec* thermal emission models. Metal abundances are measured relative to the solar photospheric values of Anders & Grevesse (1989). Galactic photoelectric absorption was incorporated using the *wabs* model (Morrison & McCammon 1983). Spectral channels were grouped to have at least 20 counts per channel. Energy ranges were restricted to 0.5–7.0 keV. The spectral fitting errors are at 1 σ confidence level, unless stated otherwise. In no case the central AGN was strongly active but, to be conservative, the central X-ray source was excluded in all spectral fittings. The correspondence between abundance ratios and SN Ia/II Fe mass fraction was done using the yields of Nomoto et al. (1997a,b).

3 – Results

3.1 – Overall Temperature and Abundance Distribution

In order to compare the fossil groups using a more "physical" measure and at the same time taking into account the poor photon statistics for our sample, we separated the spectroscopic analysis in two regions, an inner (cooling radius or ~0.1 r_{200}), ~100±30 h_{75}^{-1} kpc, and an outer region encompassing all the emission available out of the cooling radius, typically three times the size of the inner region. The cooling radius was estimated using the outermost IGM temperature (measured or known from previous observations) using $r_{200} = 0.88\ (T_{keV})^{1/2}\ h_{75}^{-1}$ Mpc (e.g. Evrard et al. 1996; Neumann 2005). Projected temperature and abundance profiles for the fossil groups are shown in Figure 1. It can be seen that most fossil groups show a lack of cooling cores. In fact, the only one that shows an apparent cooling core, RX J1416.4+2315, the hottest and most massive fossil group known, has, at larger scales, a temperature decline seen with XMM-Newton. As shown by Khosroshahi et al. (2006a), this unusual fossil group has a temperature "spike" near 200 kpc from the center, followed by a strong temperature decline at r > 200 kpc. This spike can be due to IGM azimuthal temperature substructures. Since we are using only two physical bins to compare fossil groups, the higher temperatures found for the outer bin in that fossil group are biased by the higher density (within that bin), high T_X spike region. T_X found in the central 100 kpc is higher than that found at r > 200kpc (with XMM) and the cooling time (t_{cool}) measured for this system was below (reaching 5 Gyr) the Hubble time (t_H) for regions < 150 kpc (Khosroshahi, et al. 2006), so that the expected level of cooling is not observed.

Given the proximity of NGC 6482 at z=0.013, to compare with the other fossil groups, we used only the inner region corresponding to the cooling radius, which roughly covers the whole ACIS-S3 field of view and has T_X=0.59±0.01 keV. Finer spatial analysis of this fossil group showed a significant central temperature enhancement going from ~0.48±0.04 keV at ~100 kpc from the center to 0.78±0.04 keV in the

central region (Khosroshahi, Jones & Ponman 2004), with $t_{cool} < t_H$ throughout the whole region. The metal abundance within that region was found to be somewhat high, 0.8±0.22 solar.

Within our binning, the IGM temperature of RX J1159+5531 is relatively constant at ~1.32±0.04 keV. This group has been analyzed in finer spatial detail previously (Vikhlinin et al. 2005) and it shows signs of a very small cool core at scales < 30 kpc, which is blurred in our binning resolution. The IGM temperature grows steadily (from 1~1.5 keV) from the outer regions towards the center up to 50 kpc, where it reaches ~2.6 keV and declines abruptly to a minimum of ~1.25 keV at the core. This fossil group also has a negative central abundance gradient (Fig.1), varying from 0.14±0.04 solar in the outer region and 0.28±0.04 solar in the cooling radius. The abundance gradient becomes steeper at smaller spatial scales achieving super solar values at < 25 kpc (Vikhlinin et al. 2005).

A previous Chandra and XMM analysis of ESO3060170 (Sun et al. 2004) has also shown the presence of a very small cold core (r < 10kpc) with T_X~1.5 keV and a flat temperature profile (T_X~2.6 keV) extending to r_{2500} (~400 kpc). Despite the apparent presence of a small nuclear cold core, the gas temperature within the cooling radius ($t_{cool} < t_H$ for r less than ~90 kpc) shows no evidence of declining for r > 10kpc. This is consistent with our measurements using coarser bins (Fig.1), with T_X ~ 2.3±0.15 keV and being roughly flat throughout. We also measure a central metal abundance gradient, where the abundance goes from 0.35±0.04 solar in the outer parts to 0.6±0.07 solar inside the cooling radius. This is also consistent with Sun et al. (2004) measurements.

RX J1340.5+4017 was the first fossil group found (Ponman et al. 1994) and often cited as the prototype fossil group. The gas temperatures found are ~1.25keV and consistent with having a flat profile throughout. The analysis given here for this fossil group has been carried out previously by Mendes de Oliveira et al. (2008) and we included in our analysis.

RX J1331.5+1108 shows a central temperature enhancement going from 0.24±0.09 keV outside the cooling radius to 0.56±0.04 keV in the central region. Abundances are very unconstrained (only 960 counts in the central region) but tend to be high, > 0.75 solar within the cooling radius. The outer region has an unknown spectral feature at ~1.8 keV, probably related to the Si calibration line and was removed from the spectral fittings.

Overall, the temperature profile of the fossil groups shown in Figure 1 do not show cooling cores (at the scale of the cooling radius) and have either a flat or centrally increasing temperature profile. The individual Fe abundance profiles show no obvious systematic trends. This is different from what is measured for groups of galaxies and poor cold clusters, which often show cooling cores, paired with central abundance enhancements (Finoguenov & Ponman 1999; White 2000; Finoguenov, Arnaud & David 2001).

3.2 – Elemental Abundance Ratios

As we mentioned before, the ratio of SN Ia/SN II Fe mass fraction in the ICM in the central regions of galaxy clusters and groups generally has higher values than those measured in the outer regions (e.g. Finoguenov et al. 2000). If secondary SN II driven winds occurred recently as a consequence of the BGG formation, one would expect this gradient to invert, i.e., a reduction of dominance from SN Ia Fe mass fraction in the IGM within the cooling radius. This could be checked through measurements of individual elemental ratios as described above. Despite the overall SN Ia ejecta dominance in fossil groups, in virtually all cases (perhaps with the exception of RX J1340.5+4017 – Mendes de Oliveira et al. 2008), there is a visible trend for a reduction of the SN Ia/SN II Fe mass fraction ratio towards the center, contrary to what is observed in groups and poor clusters of galaxies. In two fossil groups, NGC 6482 and RX

J1159+5531, photon statistics was good enough to see this gradient with statistical significance even in the individual profiles (Figs 2).

To determine an average SN Ia/SN II deficit quantitatively, we improved statistics by fitting jointly all six fossil groups using an equivalent binning (Figures 3a,b). In the joint fittings Hydrogen absorption and redshifts were fixed at the nominal values, gas temperatures were allowed to vary and the other *Vapec* elemental abundances were free to vary but tied to the corresponding values in the other groups. We also performed spectral fittings where gas temperatures were fixed at their best fit values found in the individual fittings. This worsened the fits and improved the abundance errors as expected, but the results were very similar to those fits with variable temperatures. The best fit gas temperatures, when free to vary, changed (not systematically) in average only 9% in the inner and 3% in the outer regions, respectively, from the best-fit values found in individual fittings. The statistical errors were larger than those, where temperatures were fixed, as expected. When calculating the energetics associated to heating the IGM near the core, we, conservatively, use the results from the spectral fittings where gas temperatures were allowed to vary.

The results using ratios involving O, Si, S and Fe show a systematic central enhancement of α-elements to Fe (Figure 4), indicating a central excess of SN II dominance with respect to the outer parts. The average Fe abundance profile shows a mild, but significant central enhancement. It varies from 0.25± 0.02 solar in the outer parts to 0.31±0.01solar in the central region. Using an error-weighted average over all the ratios shown, we find that, despite the overall dominance by SN Ia (99% ± 1% Fe mass fraction), the SN Ia Fe mass fraction declines towards the center of the average fossil group in our sample (85% ± 2% Fe mass fraction). If the temperature parameters are fixed to the best-fit values of their individual fittings, the central SN Ia Fe mass fraction decline is found to be even larger, with a corresponding SN Ia Fe mass fraction 79% ± 2% in the central region.

4 – Discussion & Conclusions

Velocity dispersions of fossil group galaxies are in accordance with the high X-ray gas temperatures and suggest that these systems have deep gravitational potential typical of poor galaxy clusters. This is consistent with their position in the L_X-T_X, L_X-σ and T_X-σ diagrams, similar to clusters of galaxies (Khosroshahi, Ponman & Jones 2007). Cosmological simulations suggest that they were formed at early epochs, given their high concentration parameters and magnitude gap between the central bright galaxy and the second brightest. On the other hand, the typical lack of cooling cores and the central decline of SN Ia Fe mass fraction found in this work suggests that their formation (at least of the BGG central merging) is posterior to that of normal groups. Explaining those properties through AGN activity is difficult since there are no obvious signs of strong AGN activity (or imprints in the IGM) seen in the X-ray images of fossil groups in our sample. More importantly, if an AGN mechanism is invoked to explain the fossil group characteristics, one should also explain why it does not prevent completely the cooling and change the gas enrichment signatures in regular groups and/or clusters of galaxies.

The central bright galaxies in fossil groups have disky isophotes, consistent with having been formed by "wet" (gaseous) mergers. If that is the case, one would expect that supernova II powered winds would heat the gas and inject metals in the central region of fossil groups, changing the chemistry of the IGM and this can be checked using an ensemble of individual abundance ratios. Our analysis of six fossil groups shows that, differently from normal groups and clusters of galaxies, there is a central enhancement of SN II ejecta, manifested through the decline of the Fe mass fraction ratio of SN II to SN Ia, from ~99% to ~85% as we approach the central regions. The difference is significant at >6 σ level.

Such a decrease in SN Ia/SN II ejecta ratio resulting from a wind would be accompanied by energy injection. The Fe mass injected by SN II into the IGM can be given by

$$MFe_{SNII} = 1.16 \times 10^{7} (f_{0.2})(Mgas_{11})(Z_{0.3})(ZFe_{\odot}))\, M_{\odot}$$

where $f_{0.2}$ is the Fe mass fraction injected by SNeII normalized by 0.2, $Mgas_{11}$ is the gas mass in units of 10^{11} solar masses, $Z_{0.3}$ is the XSPEC abundance in units of 0.3 solar, and $ZFe_{\odot}$ is the Fe solar abundance by number normalized to Hydrogen in units of 4.68 x 10^{-5} (photospheric). The total energy injected by these SNe is then $E_{inj} = (MFe_{SNII}/M_{Fe1SNII}) <E_{SNII}>$

$$E_{Inj} = \frac{MFe_{SNII}}{M_{Fe1SNII}} < E_{SNII} >= 1.29 \times 10^{59} \langle E_{SNII\_51} \rangle (f_{0.2})(Mgas_{11})(Z_{0.3})\left(ZFe_{\odot}\right)\left(\frac{M_{Fe1SNII}}{0.09M_{\odot}}\right)^{-1} erg$$

where E_{SNII_51} is the energy of 1 SN II in units of 10^{51} ergs and $M_{Fe1SNII}$ is the Fe mass produced by the average SN II (using a Salpeter IMF from 10 to 50 solar masses with the yields from Nomoto et al. 1997a,b). On the other hand, the energy needed to keep the IGM from cooling would be approximately $\Delta E \sim \Delta t\, L = 10^{58}\, \Delta t_9\, L_{42}$ erg, where Δt_9 is the average difference between the Hubble time and the cooling time within the cooling region in 10^9 yr and L_{42} is the X-ray luminosity in units of 10^{42} erg/s. The ratio of the energies above is then

$$\frac{E_{inj}}{\Delta E} \sim 1.3 \times 10^{1}\, \frac{\langle E_{SNII\_51} \rangle (f_{0.2})(Mgas_{11})(Z_{0.3})\left(ZFe_{\odot}\right)}{(\Delta t_9)(L_{42})\left(\frac{M_{Fe1SNII}}{0.09M_{\odot}}\right)}$$

For L_{42} ~2.2, $Mgas_{11}$~2.7, Δt_9 ~6, $f_{0.2}=Z_{0.3}=1$, which are typical for our sample, $E_{inj} \gtrsim 2\Delta E$ and the wind energy can be responsible for halting IGM cooling in fossil groups. The average supernovae rate for this secondary wind would be large (near 10 SNu), about twice as strong as that of M82. Furthermore, wet

mergers form stars, which let their imprint in the spectrum of the dominant galaxy, and we may look for this imprint using spectral synthesis techniques. For two of the central galaxies of the fossil groups in our sample, RXJ1340.6+4018 and RXJ1159+5531, there are available spectra in the SDSS database. Their spectra were analyzed through the spectral synthesis approach of Cid Fernandes et al. (2005; results available at the website of the STARLIGHT project, www.starlight.ufsc.br), which allows us to recover the star-formation history of the galaxies. The output of the spectral analysis of these two galaxies reveals that they have indeed a significant mass in stars with young (~5.4 x 10^8 $M_\odot$ for stars with ≲0.1 Gyr in the central galaxy of RXJ1159+5531) or intermediate (~6.4 x 10^9 $M_\odot$ for stars with a few Gyr, for RXJ1340.6+4018) ages.

Our results suggest that fossil groups are formed at later epochs, when the bright gaseous galaxies merge to form the BGG in disagreement with the common view of an early formation based on cosmological simulations. Reconciliation with the theoretical models is possible if the "halo" that will eventually become a fossil group is formed earlier than those that will become galaxy groups and clusters, but the BGG of fossil groups are formed later than the central galaxies of groups and cDs. A similar scenario has been put forward recently (Diaz-Gimenez, Muriel and Mendes de Oliveira 2008) in a study of the properties and merging history of the bright galaxies in simulated fossil groups extracted from the Millenium Simulation Galaxy Catalogue. However, using a classification based on bulge mass and relative masses of the progenitors, their work indicates that the mergers that formed the central BGGs in fossil groups were mostly "dry", in contradiction with the isophotal analysis of Khosroshahi, Ponman & Jones (2006b), and with our results. This discrepancy could be due to the particular semi-analytic recipe used in their work that can produce artificially high fraction of boxy elliptical than that observed (Diaz-Gimenez, Muriel and Mendes de Oliveira 2008).

The chemical analysis of the IGM in fossil groups is potentially a powerful discriminator among models for formation age of fossil groups. Current X-ray observations are very limited due to paucity of targets and the poor photon statistics. This limits the quantitative constraints that we can place on the energetic for individual systems and on competing scenarios for the formation of these systems. A larger sample of fossil groups with medium-deep X-ray exposures is a fundamental step to zero in on their nature and evolution. Hopefully, the X-ray sample of fossil groups observed will increase in the next few years, so that we will be able to shed light on the nature of these puzzling (but numerous) systems.

5 - Acknowledgements

R. Dupke acknowledges the support of NASA grants GO5-6139X, NNX06AG23G, NNX07AH55G and NNX07AQ76G and FAPESP 2006/05787-5. CMO and LSJ thanks the support received from FAPESP and CNPq. We thank Eli Rykoff for helpful discussions and Alexey Vikhlinin and Hugo Capelato for useful suggestions.

6 -References

Allen, S. et al. 2001, MNRAS, 322, 589

Anders, E., & Grevesse, N. 1989, Geochim. Cosmochim. Acta, 53, 197

Arnaud, K. A. 1996, in ASP Conf. Ser. 101, Astronomical Data Analysis Software and Systems V, ed. G. Jacoby & J. Barnes (San Francisco: ASP), 17

La Barbera, F.; de Carvalho, R. R.; de la Rosa, I. G.; Sorrentino, G.; Gal, R. R.; Kohl-Moreira, J. L. 2009, AJ, in press.

Cid Fernandes, R., Mateus, A., Sodré, L., Stasinska, G., & Gomes, J.M. 2005, MNRAS 358,363

Conselice, C.J. Gallagher, J. S. & Wyse, R. F., 2001, AJ, 122, 228

Cypriano, E., Mendes de Oliveira, C. L. & Sodré, L., 2006, AJ, 132, 514

de Plaa, J., Werner, N.; Bykov, A. M.; Kaastra, J. S.; Méndez, M.; Vink, J.; Bleeker, J. A. M.;

Bonamente, M. & Peterson, J. R, 2006, A&A, 452, 397

Diaz-Gimenez, E., Muriel, H., & Mendes de Oliveira, C. 2008, A&A, 490, 965

Dupke, R., 1998,PhD Thesis, Univ. Alabama

Dupke, R.A., & White, R.E.III 2000a, ApJ, 528, 139

_____, 2000b, ApJ, 537, 123

Dupke, R., & Arnaud, K. 2001, ApJ, 548, 141

D'Onghia, E., Sommer-Larsen, J., Romeo, A. D., Burkert, A., Pedersen, K., Portinari, L., &

Rasmussen, J., 2005, ApJ 630, L109

Ettori, S., Fabian, A. C., Allen, S. W., & Johnstone, R. M. 2002, MNRAS, 331, 635

Evrard, A., Metzler, C. & Navarro, J., 1996, ApJ 469, 494

Finoguenov, A. & Ponman, T., 1999, MNRAS, 305, 325

Finoguenov, A., David, L. & Ponman, 2000, ApJ, 544, 188

Finoguenov, A., Arnaud, M. & Ponman, T., 2001, ApJ, 555, 191

Fukazawa, Y., et al., 1998, PASJ, 50, 187

Heckman, T., Armus, L., & Miley, G. K. et al. 1990, ApJS 74, 833

Jones, L. R., Ponman, T. J., & Forbes, D. A. 200, MNRAS 312, 139

Jones, L. R., Ponman, T. J., Horton, A., Babul, A., Ebeling, H., & Burke, D. J. 2003, MNRAS 343, 627

Khochfar, S., & Burkert, A., 2005, MNRAS 359, 1379

Khosroshahi, H., Jones, L. R., & Ponman, T. J., 2004, MNRAS 349, 1240

Khosroshahi, H., Maughan, B. J., Jones, L. R., & Ponman, T. J., 2006a, MNRAS 369, 1211

Khosroshahi, H., Ponman, T. J., & Jones, L. R., & 2006b, MNRAS L372, 68

Khosroshahi, H, Ponman, T. J., & Jones, L. R 2007, MNRAS 377, 595

Lagana, T., Dupke, R. A., Sodre, L., Lima Neto, G. & Durret, F., 2008, MNRAS, in Press

Mendes de Oliveira, C., Cypriano, E. S., & Sodré, L. Jr. 2006, AJ, 131, 158

Mendes de Oliveira, C., Cypriano, E., Dupke, R. A., & Sodre, L. 2008, AJ,

Morrison, R., & McCammon, D. 1983, ApJ, 270, 119

Mulchaey, J. S., & Zabludoff, A. I., 1999, ApJ, 514,133

Mushotzky, R.F., Loewenstein, M., Arnaud, K. A., Tamura, T., Fukazawa, Y., Matsushita, K., Kikuchi, K., & Hatsukade, I. 1996, ApJ, 466, 686

Neumann, D.M., 2005, A&A 439, 465

Nomoto, K., Hashimoto, M., Tsujimoto, T., Thielemann, F.-K., Kishimoto, N., Kubo, Y., & Nakasato, N., 1997, Nuc. Phys. A, A616, 79

Nomoto, K., Iwamoto, K., Nakasato, N., Thielemann, F.-K., Brachwitz, F., Tsujimoto, T., Kubo, Y., & Kishimoto, N., 1997, Nuc. Phys. A, A621, 467

Ponman, T., Allan, D. J., Jones, L. R., Merrifield, M., McHardy, I. M., Lehto, H. J., & Luppino, G. A.1994 Nature 369, 462

Rasera, Y, Lynch, B., Srivastava, K. & Chandran, B. 2008, ApJ, 689, 825

Rasmussen, J. & Ponman, T. J. 2007, MNRAS 380, 1554

Sun, M., Forman, W., Vikhlinin, A, Hornstrup, A., Jones, C., & Murray, S. S., 2004, ApJ, 612, 805

Strickland, D., Heckman, T. M., Colbert, E. J. M., Hoopes, C. G., & Weaver, K. A., 2004, ApJ, 606, 829

Van Dokkum, P., Franx, M., Fabricant, D., Kelson, D. D., & Illingworth, G. D. 1999, 520, L95

Vikhlinin, A., McNamara, B. R., Hornstrup, A., Quintana, H., Forman, W., Jones, C., & Way, M. 1999, ApJ, 520, L1

Vikhlinin, A., Markevitch, M., Murray, S. S., Jones, C., Forman, W., & Van Speybroeck, L., 2005, ApJ, 628, 655

Wechsler, R. H., Bullock, J. S., Primack, J. R., Kravtsov, A. V., & Dekel, A., 2002, ApJ, 568, 52

White, D. A., 2000, MNRAS 312, 663

Zibetti, S., Pierini, D., & Pratt, G.W. 2009, MNRAS 392, 525

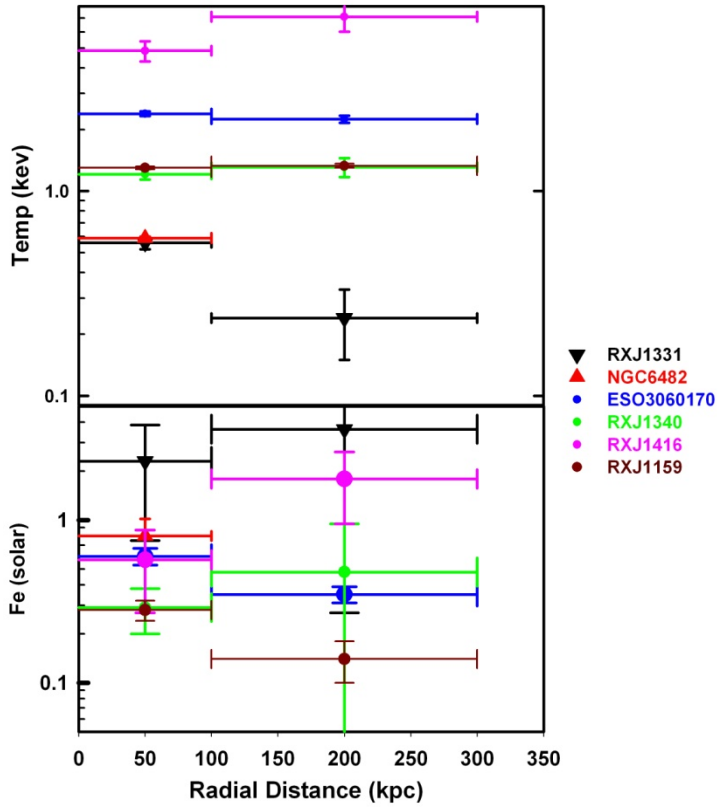

Figure 1(Left) - Temperature and abundance profiles for the fossil groups analyzed here. The spectral model is an absorbed (*wabs*) *Apec*. The spatial binning separates an inner (~cooling radius) region from the outer region. Errors are at the 1-σ confidence level. Fossil group names are color coded.

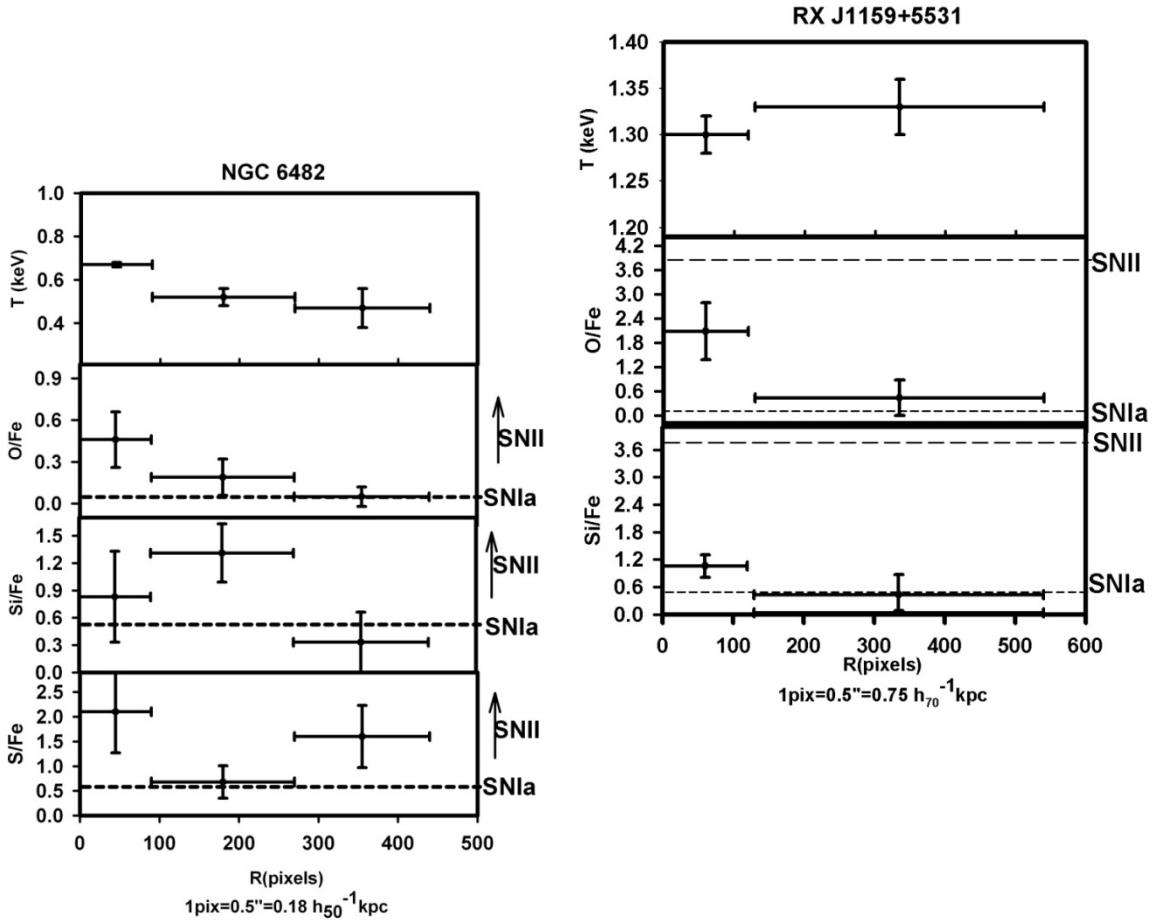

Figure 2(a) – Temperature and abundance ratio profiles involving O, Si, S and Fe for the fossil group NGC 6482. The short-dotted lines show the values corresponding to 100% SN Ia Fe mass fraction dominance. The higher the values the closer to SN II dominance. Errors show the 1-σ confidence level. **(b)** same as (a) but for RX J1159+5531. Long dashed lines indicate the values corresponding to 100% SN II enrichment. Yields taken from

Nomoto et al. (1997a,b).

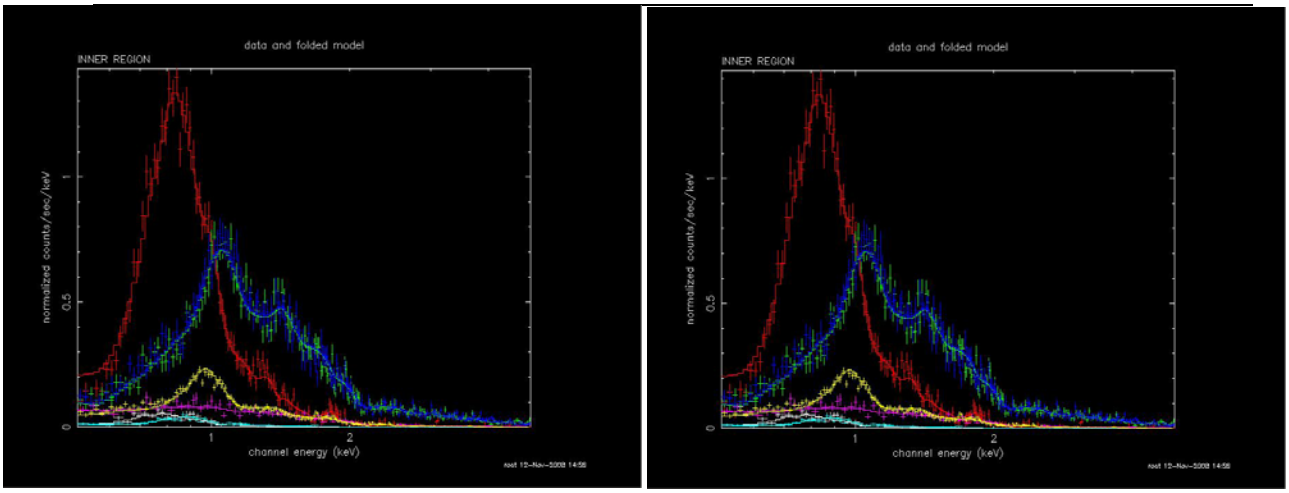

Figure 3(a) – Spectra and best fit model for the joint fit of all fossil groups for the inner region shown in Figure 4.

(b) Same for the outer region (without NGC 6482).

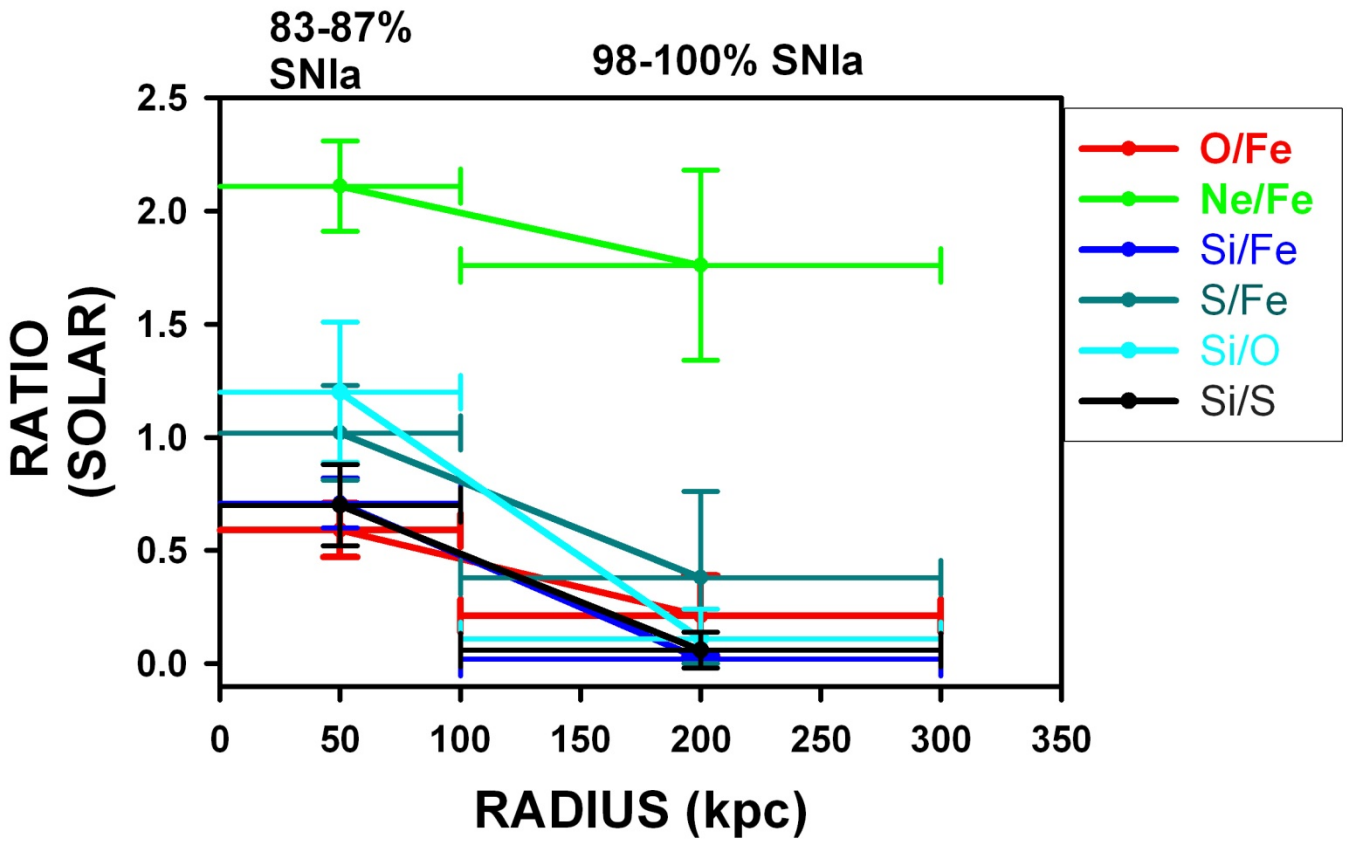

Figure 4 – Abundance ratio profiles for the "average" fossil group. Individual abundance ratios are color coded. A connecting line for the profile for each ratio is plotted for clarity. The inner region corresponds to an error weighted SN Ia Fe mass fraction of 0.85±0.02 and the outer region to SN Ia Fe mass fraction of 0.99±0.01. Spectral model is an absorbed *Vapec* and allows individual gas temperatures to vary. 1-σ errors are shown.